Contribution from the Department of Chemistry,
University of Houston—University Park, Houston, Texas 77004

Electrochemistry and Spectroelectrochemistry of Easily Reducible and Easily Oxidizable Iron Porphyrins. Reactions of Monomeric and Dimeric Pyrrole-Substituted Tetracyano and Phenyl-Substituted Diethylamino Complexes of Iron Tetraphenylporphyrins

K. M. KADISH,* B. BOISSELIER-COCOLIOS, B. SIMONET, D. CHANG, H. LEDON,† and P. COCOLIOS†

Received December 11, 1984

The electrochemistry of monomeric and dimeric iron tetraphenylporphyrins substituted at the pyrrole position by electron-withdrawing CN groups or at the phenyl position by electron-donating diethylamino groups was investigated in nonaqueous media. The presence of electron-withdrawing CN groups on the pyrrole ring produced large positive shifts of reduction potentials such that, for the case of $[(CN)_4TPP]FeCl$, reduction of iron(II) could be accomplished at −0.42 V vs. SCE. Similar negative shifts were also observed for $[[(CN)_4TPP]Fe]_2O$, and this compound could be easily reduced in four one-electron-transfer steps without destruction of the dimer. In contrast, the presence of diethylamino substituents led to large negative shifts of oxidation potentials. For the case of $[(p\text{-}Et_2N)TPP]FeCl$ in benzonitrile, four oxidation processes were observed, with the first occurring at 0.61 V vs. SCE. The electron-transfer processes of each compound were monitored by ESR and UV-visible spectroscopy, and an overall oxidation-reduction scheme was formulated. No evidence for generation of iron(IV) was observed. However, based on ESR results the generation of iron(I) porphyrin complexes was clearly indicated.

Introduction

Numerous electrochemical studies of synthetic iron porphyrins have appeared in the literature during the last two decades.[1-3] The physical and chemical properties of many simple porphyrins containing the iron(II) and iron(III) oxidation state are now well characterized, and more attention has recently been devoted toward elucidating the properties of highly oxidized[4-9] or highly reduced complexes.[10-12] In this regard, prior controversies regarding the site of oxidation appear to be resolved only for the simple complexes of iron tetraphenylporphyrins or iron octaethylporphyrins where it now appears certain that the first and second oxidations of these species generate cation radicals and dications rather than an iron(IV) and an iron(IV) cation radical, respectively.[5]

Less clear-cut are assignments for the first reduction product of Fe(II). The present state of understanding in this area has been very nicely summarized by Reed[12] who concluded that the best formulation of the reduced complex is one that involves delocalization of charge between an Fe(II) anion radical and an Fe(I) anion. This conclusion, however, is not generally quoted in the literature, and formalisms involving pure Fe(I) or pure anion radical character are still routinely given in current publications.

One of the original postulates for electrochemical generation of iron(I) was made by our own laboratory.[13] This characterization was made primarily on earlier ESR evidence[14] that, by itself, clearly rules against radical anion formation. In this paper we have reinvestigated the ESR of reduced Fe(II) porphyrins but have utilized the more easily reducible tetracyano-substituted complex of iron tetraphenylporphyrin. Preliminary electrochemical results of this compound have been reported,[15] but as will be demonstrated in this paper, the characterized compound was actually the μ-oxo dimer rather than the intended monomeric $[(CN)_4TPP]FeCl$.

The electrochemistry of numerous metalloporphyrins containing tetracyano substituents has demonstrated that positive shifts in $E_{1/2}$ as large as 1.0 V can be achieved with respect to potentials of the unsubstituted tetraphenylporphyrins with the same metal.[15-17] Thus, it was anticipated that electrogeneration of Fe(I), or the anion radical, from $[(CN)_4TPP]FeCl$ would occur at potentials more positive than −0.5 V vs. SCE. This indeed is the case as we report in this study of monomeric $[(CN)_4TPP]FeCl$ and dimeric $[[(CN)_4TPP]Fe]_2O$. The shift of reduction potentials in a positive direction enables additional reductions to be observed within the potential range of the electrochemical solvent (≈−2.0 V vs. SCE), and it was anticipated that the generation of Fe(I) after formation of an Fe(II) anion or dianion might also be achievable, as was the case for copper(II) tetracyanotetraphenylporphyrin.[18]

The oxidation of iron μ-oxo dimers containing highly electron-donating substituents has been reported.[19] Addition of diethylamino groups to the four phenyl rings of $((TPP)Fe)_2O$ leads to marked negative shifts in oxidation potentials and facilitates the electrochemical generation of highly oxidized species at very negative potentials. The first two oxidations of $[[(p\text{-}Et_2N)TPP]Fe]_2O$ occur at 0.34 and 0.47 V, but only radical cations and dications are generated.[19] In this paper we report the electroreduction of this same compound as well as the electrooxidation and electroreduction of $[(p\text{-}Et_2N)TPP]FeCl$. It was hoped that the negative shift of potentials resulting from the diethylamino groups might induce a change from a ring-centered to a metal-centered oxidation of Fe(III), or if this did not occur, at the very least it was hoped that generation of Fe(IV) after cation radical or dication formation could be investigated in the potential range of the electrochemical solvents.

† Present address: L'Air Liquide, CRCD, F-78350 Jouy-en-Josas, France.

(1) See references in: Kadish, K. M. In "Iron Porphyrins", Part II; Lever, A. B. P., Gray, H. B., Eds.; Addison-Wesley: Reading, MA, 1982; Chapter 4.
(2) See references in: Bottomley, L. A.; Olson, L.; Kadish, K. M. In "Electrochemical and Spectrochemical Studies of Biological Redox Components"; Kadish, K. M., Ed.; American Chemical Society: Washington, DC, 1982; Adv. Chem. Ser. No. 201, p 279.
(3) See references in: Kadish, K. M. *J. Electroanal. Chem. Interfacial Electrochem.* **1984**, *168*, 261.
(4) Philippi, M. A.; Goff, H. M. *J. Am. Chem. Soc.* **1982**, *104*, 6026.
(5) Goff, H. M.; Philippi, M. A. *J. Am. Chem. Soc.* **1983**, *105*, 7567.
(6) LaMar, G. N.; de Ropp, J. S.; Latos-Grazynski, L.; Balch, A. L.; Johnson, R. B.; Smith, K. M.; Parish, D. N.; Cheng, R.-J. *J. Am. Chem. Soc.* **1983**, *105*, 782.
(7) English, D. R.; Hendrickson, D. N.; Suslick, K. S. *Inorg. Chem.* **1983**, *105*, 782.
(8) Hofmann, J. A., Jr.; Bocian, D. F. *Inorg. Chem.* **1984**, *23*, 1177.
(9) Gans, P.; Marchon, J. C.; Reed, C. A.; Regnard, J. R. *Nouv. J. Chim.* **1981**, *5*, 201.
(10) Collman, J. P.; Sorell, T. N.; Dawson, J. H.; Trudel, J. R.; Bunnenburg, E.; Djerassi, C. *Proc. Natl. Acad. Sci. U.S.A.* **1976**, *73*, 6.
(11) Welborn, C. H.; Dolphin, D.; James, B. R. *J. Am. Chem. Soc.* **1981**, *103*, 2869.
(12) Reed, C. A. In "Electrochemical and Spectrochemical Studies of Biological Redox Components"; Kadish, K. M., Ed.; American Chemical Society: Washington, DC; 1982; Adv. Chem. Ser. No. 201, p 333.
(13) Kadish, K. M.; Larson, G.; Lexa, D.; Momenteau, M. *J. Am. Chem. Soc.* **1975**, *97*, 282.
(14) Cohen, I. A.; Ostfeld, D.; Lichenstein, B. *J. Am. Chem. Soc.* **1972**, *94*, 4552.
(15) Giraudeau, A.; Callot, H. J.; Jordan, J.; Ezhar, I.; Gross, M. *J. Am. Chem. Soc.* **1979**, *101*, 3857.
(16) Giraudeau, A.; Callot, H. J.; Gross, M. *Inorg. Chem.* **1979**, *18*, 201.
(17) Callot, H. J.; Giraudeau, A.; Gross, M. *J. Chem. Soc., Perkin Trans. 1* **1975**, *2*, 1321.
(18) Giraudeau, A.; Louati, A.; Gross, M.; Callot, H. J.; Hanson, L. K.; Rhodes, R. K.; Kadish, K. M. *Inorg. Chem.* **1982**, *21*, 1581.
(19) Chang, D.; Cocolios, P.; Wu, Y. T.; Kadish, K. M. *Inorg. Chem.* **1984**, *23*, 1633.

0020-1669/85/1324-2148$01.50/0

Table I. Summary of Half-Wave Potentials (V vs. SCE) of (P)FeCl in CH_2Cl_2 (0.1 TBAP) [P = $(CN)_4TPP$ or TPP]

		oxidation		reduction			
compd	solvent	$E_{1/2}^{II}$(ox)	$E_{1/2}^{I}$(ox)	$E_{1/2}^{I}$(red)	$E_{1/2}^{II}$(red)	$E_{1/2}^{III}$(red)	E_{pc}^{IV}(red)
$[(CN)_4TPP]FeCl$	CH_2Cl_2	1.8[a]	1.43	0.17	−0.42	−0.83	−1.83[b]
	DMF			0.17	−0.43	−0.82	
(TPP)FeCl	CH_2Cl_2[c]	1.40	1.14	−0.23	−1.07	−1.60	
	DMF[d]		1.17	−0.19	−1.03	−1.61	

[a] Anodic peak potential, E_{pa}, at 100 mV/s. [b] Cathodic peak potential, E_{pc}, at 100 mV/s. [c] Reference 24. [d] Reference 13.

Experimental Section

Instrumentation. ESR spectra were recorded on an IBM Model ER 100D spectrometer equipped with an ER 040-X microwave bridge and an ER 080 power supply. ^1H NMR spectra were recorded on a Varian XL-100 spectrometer. Spectra were measured from 10-mg solutions of each complex in 0.5 mL of $CDCl_3$ with tetramethylsilane as internal reference. IR spectra were performed on a Perkin-Elmer 1330 spectrophotometer. Samples were 1% dispersions in CsI pellets. UV–visible spectra were recorded on a Tracor Northern 1710 holographic optical spectrometer/multichannel analyzer or an IBM 9430 spectrophotometer.

Cyclic voltammetric measurements were obtained with the use of a three-electrode system with an EG&G Model 173 potentiostat, an EG&G Model 175 universal programmer, and a Houston Instruments Model 2000 X-Y recorder or a BAS-100 electrochemical analyzer, a Houston Instruments HIPLOT DMP-40 plotter, and an EPSON Model FX 80 printer. The working electrode was a platinum button, and a platinum wire served as a counter electrode. A saturated calomel electrode (SCE) was used as the reference electrode and was separated from the bulk of the solution by a fritted-glass bridge.

Controlled-potential electrolysis was performed in a bulk cell where the SCE reference electrode and the platinum-wire counter electrode were separated from the test solution by fritted bridges containing solvent and supporting electrolyte. An EG&G Model 173 potentiostat or a BAS-100 electrochemical analyzer were used to control the potential.

Thin-layer spectroelectrochemical measurements were performed with an IBM Model EC225 voltammetric analyzer coupled with a Tracor Northern 1710 holographic optical spectrometer/multichannel analyzer to obtain time-resolved spectral data. The thin-layer cell consisted of a 1000-lpi gold minigrid electrode sandwiched between two glass slides as previously described.[20]

Chemicals. Methylene chloride (CH_2Cl_2) was first distilled from P_2O_5 and then CaH_2 prior to use. Dimethylformamide (DMF) was distilled over $MgSO_4$ under reduced pressure. Benzonitrile (PhCN) was distilled under reduced pressure over P_2O_5. Tetrabutylammonium perchlorate (TBAP) (Fluka) was recrystallized from ethanol. Tetrabutylammonium hexafluorophosphate ($(TBA)PF_6$) (Fluka) was recrystallized from ethyl acetate.

[(*p*-Et_2N)TPP]$Fe]_2O$ was prepared according to a previously described method[19] and exhibited the following characteristics. UV–vis (CH_2Cl_2) λ, nm (ε × 10^{-3}): 450 (45.1), 587 (13.2), 642 (5.7). IR (CsI pellet): $\nu_{Fe-O-Fe}$ = 900 and 885 cm^{-1}. ^1H NMR ($CDCl_3$): δ_{pyr-H} = 13.4, δ_{Ph-H} = 7.3, δ_{CH_2} = 3.65, δ_{CH_3} = 1.45.

[(*p*-Et_2N)TPP]FeCl was obtained by reaction of the dimer with HCl gas.[19] UV–vis (CH_2Cl_2) λ, nm (ε × 10^{-3}): 375 (23.5), 453 (51.0), 551 (14.1), 736 (3.8). IR (CsI pellet): ν_{Fe-Cl} = 355 cm^{-1}. ^1H NMR ($CDCl_3$): δ_{pyr-H} = 78.3 δ_{m-H} = 5.41, δ_{CH_2} = 5.41, δ_{CH3} = 1.91. ESR (115 K): $g_\parallel$ = 2.02, $g_\perp$ = 5.85.

Free base $[(CN)_4TPP]H_2$ was synthesized according to the method described by Callot,[21] and insertion of iron into the porphyrin core was accomplished using the method described by Giraudeau et al.[15] However, as noted above, the species electrochemically investigated in an earlier study was actually the μ-oxo dimer, $[[(CN)_4TPP]Fe]_2O$. The physicochemical properties of the metalated compounds are as follows:

$[(CN)_4TPP]FeCl$. UV–vis (CH_2Cl_2) λ, nm (ε × 10^{-3}): 380 (30.0), 444 (76.0), 601 (51.2), 629 (14.2). IR (CsI pellet): ν_{Fe-Cl} = 360 cm^{-1}. ^1H NMR ($CDCl_3$): δ_{pyr-H} = 77, δ_{o-H} = 12.74, δ_{m-H} = δ_{p-H} = 1.45. ESR (115 K): $g_\parallel$ = 2.01, $g_\perp$ = 5.79.

$[(CN)_4TPP]Fe]_2O$. UV–vis (CH_2Cl_2) λ, nm (ε × 10^{-3}): 440 (41.1), 665 (12.3), 690 (8.0). IR (CsI pellet): $\nu_{Fe-O-Fe}$ = 860 cm^{-1}. Due to the dimer's insolubility or very low solubility in most solvents, no NMR spectrum was recorded.

Results and Discussion

Electrooxidation–Reduction of $[(CN)_4TPP]FeCl$. Typical cyclic voltammograms of $[(CN)_4TPP]FeCl$ in CH_2Cl_2 and DMF are given in Figure 1. Four reductions (at $E_{1/2}$ = +0.17, −0.42, and −0.83 V and E_{pc} = −1.83 V (not shown in figure)) and two oxidations (at $E_{1/2}$ = +1.43 V and E_{pa} = +1.8 V) are observed in CH_2Cl_2 while in DMF, which has a less positive potential range, no oxidation could be observed. Potentials for all of the measured reactions are summarized in Table I which also includes potentials for the oxidation–reduction of (TPP)FeCl. Values of $E_{1/2}$ were determined by cyclic voltammetry and by rotating-disk voltammetry and were identical within experimental error. Very surprisingly, potentials for the reduction of $[(CN)_4TPP]FeCl$ are identical in CH_2Cl_2 and DMF, suggesting that little or no ligand interaction occurs between DMF molecules and the neutral or reduced species.

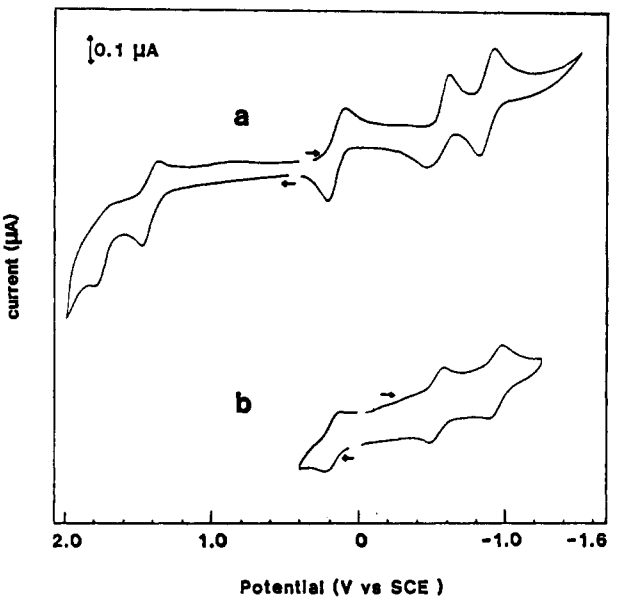

Figure 1. Cyclic voltammograms of $[(CN)_4TPP]FeCl$ in (a) CH_2Cl_2 (0.1 M TBAP) and (b) DMF (0.1 M TBAP) [scan rate 100 mV/s].

It is interesting to note that half-wave potentials for the first and second reductions of $[(CN)_4TPP]FeCl$ are separated by 600 mV in DMF ($E_{1/2}$ = +0.17 and −0.43 V) while the first and second reductions of (TPP)FeCl (at $E_{1/2}$ = −0.19 and −1.03 V) are separated by 840 mV in the same solvent. In addition, half-wave potentials for the second and third reductions of $[(CN)_4TPP]FeCl$ are separated by 390 mV as compared to a 580 mV difference between $E_{1/2}^{II}$ and $E_{1/2}^{III}$ for (TPP)FeCl in DMF. These differences in reduction potentials between the two compounds are clearly related to differing effects of the electron-withdrawing cyano substituents on each electroreduction.

Detailed electrochemical studies of tetracyano- and other pyrrole-substituted tetraphenylporphyrins have shown that a larger substituent effect is observed for reductions than for oxidations of the metalloporphyrin π-ring system.[16] In addition, the smallest substituent effect (i.e., shift of half-wave potentials) is present for electrode reactions involving the central metal of a metalloporphyrin.[15,22] The oxidation–reduction potentials of $[(CN)_4TPP]FeCl$ also appear to follow this trend. Potentials for the first two oxidations of $[(CN)_4TPP]FeCl$ in CH_2Cl_2 ($E_{1/2}$ = 1.45 V and E_p = 1.8 V) are shifted by 310 and 400 mV with respect to

(20) Rhodes, R. K.; Kadish, K. M. *Anal. Chem.* **1981**, *53*, 1539.
(21) Callot, H. J. *Bull. Soc. Chim. Fr.* **1974**, 1492.
(22) Kadish, K. M.; Morrison, M. M. *Inorg. Chem.* **1976**, *15*, 980.

Table II. Maximum Absorbance Wavelengths (λ_{max}) and Corresponding Molar Absorptivities (ϵ) for $[(CN)_4TPP]FeCl$ in CH_2Cl_2 (0.5 M TBAP)

pot. of electrogenern, V	abs species[a]	solvent	λ_{max}, nm ($\epsilon \times 10^{-3}$)			
none	$[(CN)_4TPP]FeCl$	CH_2Cl_2	380 (30.0)	444 (76.0)	601 (15.2)	629 (14.2)
		DMF	425 (36.2)	452 (74.5)	598 (15.6)	628 (15.1)
none	$[(CN)_4TPP]FeClO_4$	CH_2Cl_2		445 (75.2)	670 (21.3)	
+0.0	$[[(CN)_4TPP]Fe]$	CH_2Cl_2	451 (75.6)	476 (139.8)	673 (28.9)	717 (32.3)
		DMF	450 (62.8)	476 (72.4)	673 (10.2)	720 (10.3)
−0.50 to −0.75	$[[(CN)_4TPP]Fe]^-$	CH_2Cl_2	435 (38.3)	472 (45.3)	599 (30.2)	828 (24.8)
		DMF		481 (43.8)	576 (6.0)	620 (11.1)
−1.20	$[[(CN)_4TPP]Fe]^{2-}$	CH_2Cl_2		457 (44.4)	570 (30.4)	619 (49.5)

[a] Cl^- ion not shown as associated to reduced species.

half-wave potentials for the oxidation of (TPP)FeCl (at $E_{1/2}$ = 1.14 and 1.40 V) in the same solvent. This is consistent with the 350–570 mV difference in half-wave potentials between $[(CN)_4TPP]Cu$ and (TPP)Cu or between $[(CN)_4TPP]H_2$ and $(TPP)H_2$. Potentials for the second and third reduction of $[(CN)_4TPP]FeCl$ in DMF (at $E_{1/2}$ = −0.43 and −0.82 V) are shifted by 600 and 790 mV with respect to those for the same electrode reactions of (TPP)FeCl (at $E_{1/2}$ = −1.03 and −1.61 V). The first of these reactions could involve either the π-ring system or the orbitals of the central metal[12] while the second (for the case of (TPP)FeCl) involves the π-ring system. Finally, the substituent effect of the CN groups on the first reduction of $[(CN)_4TPP]Fe$ is the most reduced in magnitude. The shift in $E_{1/2}$ with respect to (TPP)FeCl for the first reduction is only 360 mV in DMF, although a larger shift of 400 mV is observed in CH_2Cl_2.

Great care must be taken when using electrochemical substituent effects to indicate the site of metalloporphyrin electrooxidation or electroreduction. Comparisons between series of compounds can be used to suggest reaction sites,[22] but any conclusions must be confirmed by other physicochemical measurements. In this regard it is clearly established that the first reduction of (TPP)FeCl and $[(CN)_4TPP]FeCl$ involves an Fe(III)/Fe(II) transition, and substituent effects for this electroreduction are greatly reduced in magnitude from those of known π-ring-centered reactions. The electrochemical reduction of $(TPP)Co^{II}$ also involves a metal-centered reduction, and when compared to $[(CN)_4TPP]Co^{II}$ reduction in DMF, a positive shift of 565 mV is noted.[15] This shift of $E_{1/2}$ due to the four CN groups on $[(CN)_4TPP]Co^{II}$ is very similar to that for reduction of $[(CN)_4TPP]Fe^{II}$ in DMF and may be due to a similarity of the reduction site, which for the case of (TPP)Co is metal centered and for the case of (TPP)FeCl has been postulated to be partially[12] or wholely[13] metal centered.

Spectroscopic Characterization of $[(CN)_4TPP]FeCl$ Reduction Products. Controlled-potential electrolysis and time-resolved electronic absorption spectra or ESR spectra were recorded after each electroreduction step. Application of a controlled potential of −0.01 V generated a typical Fe(II) spectrum with a red-shifted Soret band as shown in Figure 2. Back-electrolysis at a controlled potential of +0.4 V did not lead to the initial spectrum but rather to the identified Fe(III) spectrum of $[(CN)_4TPP]FeClO_4$[23] as depicted in Figure 3 and Table II. Generation of the perchlorate salt upon back-electrolysis is not unexpected[24] since TBAP was present at 0.5 M while only millimolar Cl^- existed in solution.

Of most interest are the electronic absorption spectra and ESR spectra registered after the second reduction of $[(CN)_4TPP]FeCl$. Controlled-potential electrolysis at −0.5 V showed the addition of 1.0 electron and generated the radical-like spectrum shown in Figure 4a. No intermediates were observed in this reduction, and back-electrolysis produced the original Fe(II) species. The neutral $[(CN)_4TPP]FeCl$ has an ESR spectrum with signals at g = 5.79 and 2.00 (see Figure 5a) and is typical of high-spin Fe(III).[25] Upon electroreduction in CH_2Cl_2 at −0.01 V this signal

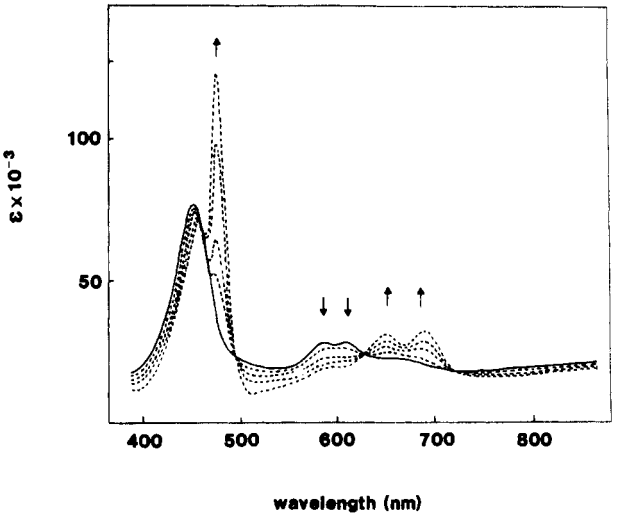

Figure 2. Time-resolved electronic absorption spectrum of $[(CN)_4TPP]Fe^{II}$ electro-generated in an OTTLE at a controlled potential of −0.01 V in CH_2Cl_2 (0.5 M TBAP).

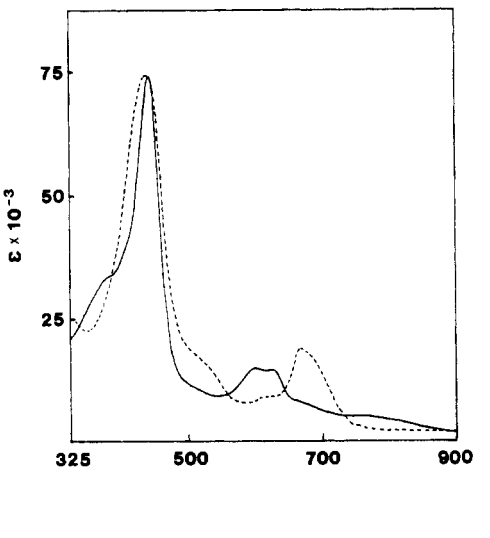

Figure 3. Electronic absorption spectra of $[(CN)_4TPP]FeCl$ (—) and $[(CN)_4TPP]FeClO_4$ (---) in CH_2Cl_2 (0.5 M TBAP).

disappeared as the d^6 Fe(II) was generated. Further reduction at potentials between −0.42 and −0.83 V lead to the ESR spectrum shown in Figure 5b. This spectrum shows three lines at g = 2.03, 2.00, and 1.98, and its width is of 160 G. Although these g values are all near g_e, values of 2.03 and 1.98 are still indicative of substantial electron density on the metal center. The formalism

(23) Genuine samples of $[(CN)_4TPP]FeClO_4$ were synthesized by reaction of $[(CN)_4TPP]FeCl$ with $AgClO_4$. Identification of $[(CN)_4TPP]FeClO_4$ was by its UV–visible spectra and the characteristic IR stretching frequencies of ClO_4.

(24) Bottomley, L. A.; Kadish, K. M. *Inorg. Chem.* **1981**, *20*, 1348.

(25) Palmer, G. In "Iron Porphyrins", Part II; Lever A. B. P., Gray, H. B., Eds.; Addison-Wesley: Reading, MA, 1982; Chapter 2.

(26) Lexa, D.; Momenteau, M.; Mispelter, J. *Biochim. Biophys. Acta* **1974**, *338*, 151.

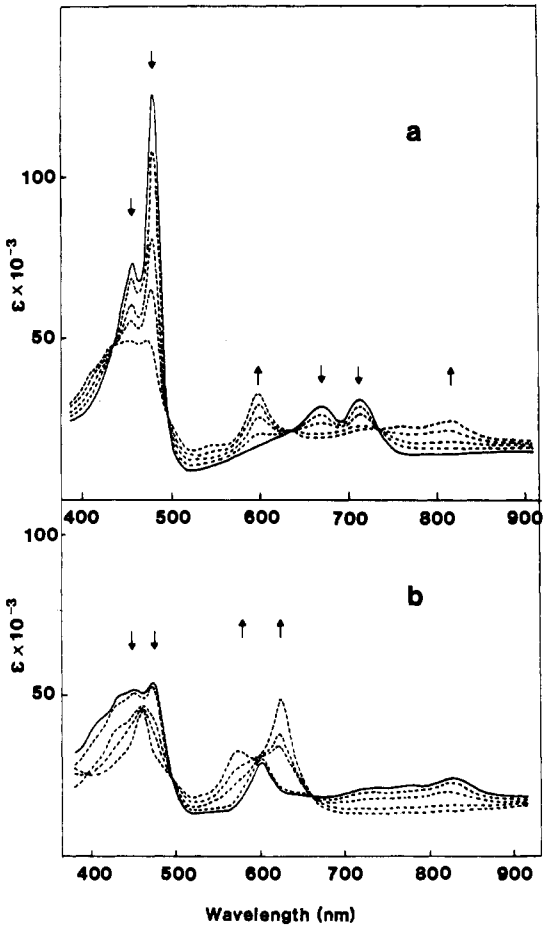

Figure 4. Time-resolved electronic absorption spectra of (a) $[[(CN)_4TPP]Fe]^-$ generated at −0.75 V and (b) $[[(CN)_4TPP]Fe]^{2-}$ generated at −1.20 V. Both spectra were taken in CH_2Cl_2 (0.5 M TBAP) with an OTTLE. Initial species are represented by a solid line.

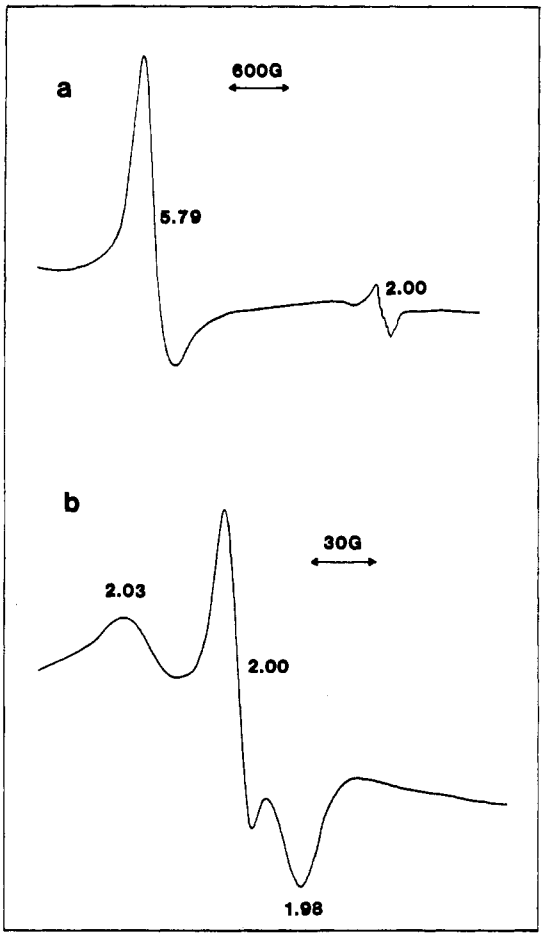

Figure 5. ESR spectra of (a) $[(CN)_4TPP]FeCl$ and (b) $[[(CN)_4)-TPP]Fe]^-$ generated at −0.75 V, recorded at 110 K.

described by Reed[12] still applies, but the doubly reduced species appears to present more anion radical characteristics than Fe(I) characteristics.

Finally, addition of a third electron to $[(CN)_4TPP]FeCl$ leads to a species with a well-defined UV–visible spectrum that is very similar to that of a chlorin.[27] This is shown in Figure 4b, and the wavelength maxima are summarized in Table II. As seen in this figure and table, the Soret band of $[[(CN)_4TPP]Fe]^{2-}$ has totally disappeared and only three major peaks are present at 457, 570, and 619 nm. No intermediates are observed in either the time-or the potential-resolved spectra, and regeneration of the neutral $[(CN)_4TPP]Fe^{II}$ spectrum could be accomplished by reversing the potential to 0.0 V.

Electrochemistry of $[[(CN)_4TPP]Fe]_2O$. The electroreduction behavior of $[[(CN)_4TPP]Fe]_2O$ is quite different from that reported for $((TPP)Fe)_2O$[13,28] or $((OEP)Fe)_2O$.[29] Unlike all other iron μ-oxo dimers, the tetracyano complex undergoes four reversible one-electron-transfer additions without cleavage of the dimer. This is shown in Figure 6 which illustrates a cyclic voltammogram and differential-pulse voltammogram of $[[(CN)_4TPP]Fe]_2O$ in a saturated DMF solution containing 0.1 M TBAP. Although the currents are low by cyclic voltammetry (due to the low solubility of the complex in DMF), measurements of peak potentials are possible and indicate a reversible one-electron-transfer separation ($E_{pa} - E_{pc} = 60 \pm 10$ mV). The shapes of the differential-pulse voltammograms are also indicative of

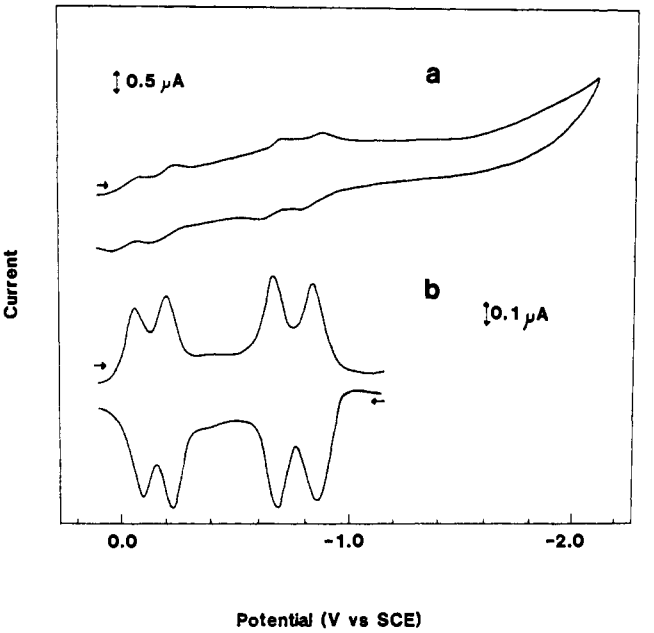

Figure 6. (a) Cyclic voltammogram of saturated $[[(CN)_4TPP]Fe]_2O$ in DMF (0.1 M TBAP) at 100 mV/s and (b) differential-pulse voltammogram of the same compound at 4 mV/s.

diffusion-controlled one-electron transfers ($w_{1/2} = 110 \pm 10$ mV). More significant, however, are the heights and potentials of the peaks by reverse differential-pulse voltammetry. These current–voltage curves are shown in Figure 6b and clearly demonstrate the reversibility of all four processes as well as the stability of the μ-oxo dimer after total electroreduction to $[[[(CN)_4TPP]Fe]_2O]^{4-}$.

(27) Fajer, J.; Borg, D. C.; Forman, A.; Felton, R. H.; Dolphin, D.; Vegh, L. *Proc. Natl. Acad. Sci. U.S.A.* **1974**, *71*, 994.
(28) Kadish, K. M.; Cheng, J.; Cohen, I. A.; Summerville, D. *ACS Symp. Ser.* **1977**, *No. 38*, 65.
(29) Stolzenberg, A. M.; Strauss, S. H.; Holm, R. H. *J. Am. Chem. Soc.* **1981**, *103*, 4763.

Table III. Half-Wave Potentials (V vs. SCE) of [(*p*-Et_2N)TPP]FeCl in Various Solvent/Supporting Electrolyte Mixtures

		oxidation				reduction	
solvent	supp electrolyte	$E_{1/2}^{IV}$(ox)	$E_{1/2}^{III}$(ox)	$E_{1/2}^{II}$(ox)	$E_{1/2}^{I}$(ox)	E_p^{I}(red)[a]	$E_{1/2}^{II}$(red)
CH_2Cl_2	(TBA)PF_6	1.34[c]	1.14[c]	0.74	0.58	−0.48	−1.18
PhCN	(TBA)PF_6	1.33[c]	1.10[c]	0.73	0.59	−0.48	−1.17
CH_2Cl_2	TBAP	1.31[c]	1.16[c]	0.78	0.61	−0.42	−1.13
DMF	TBAP	*b*	1.08[d]		0.66[c]	−0.34	−1.11
Me_2SO	TBAP	*b*	*b*		0.65[c]	−0.19	−1.20

[a] Cathodic reduction peak at 100 mV/s. [b] Reaction occurs beyond potential range of solvent. [c] Two-electron transfer. [d] Irreversible oxidation.

The four reductions of [[(CN)$_4$TPP]Fe]$_2$O occur at $E_{1/2}$ = −0.07, −0.22, −0.69, and −0.87 V and correspond to the following series of electrode reactions:

$$[[(CN)_4TPP]Fe]_2O + e^- \rightleftarrows [[[(CN)_4TPP]Fe]_2O]^- \quad (1)$$

$$[[[(CN)_4TPP]Fe]_2O]^- + e^- \rightleftarrows [[[(CN)_4TPP]Fe]_2O]^{2-} \quad (2)$$

$$[[[(CN)_4TPP]Fe]_2O]^{2-} + e^- \rightleftarrows [[[(CN)_4TPP]Fe]_2O]^{3-} \quad (3)$$

$$[[[(CN)_4TPP]Fe]_2O]^{3-} + e^- \rightleftarrows [[[(CN)_4TPP]Fe]_2O]^{4-} \quad (4)$$

It is suggested that the first two reductions correspond to the initial formation of a mixed-oxidation-state Fe(III)–Fe(II) dimer followed by formation of an Fe(II)–Fe(II) dimer after addition of a second electron. This assignment is based on ESR results for the reduction of ((TPP)Fe)$_2$O in DMF, which indicates the transient formation of a mixed-oxidation-state dimer after the addition of one electron.[13] The addition of four electrons to [[(CN)$_4$TPP]Fe]$_2$O without cleavage of the dimer may be compared to results for the oxidation of [[(*p*-Et_2N)TPP]Fe]$_2$O where four electrons can be extracted in a stepwise manner while preserving the dimeric structure of the complex.[19] However, for the oxidations of [[(*p*-Et_2N)TPP]Fe]$_2$O, all reactions appear to be ring centered. This is probably not the case for [[(CN)$_4$TPP]-Fe]$_2$O where at least two, if not four, electrons can be added to the iron center. Finally, it is interesting to note that the substituent effect due to the addition of eight CN groups to ((TPP)Fe)$_2$O is similar to that for the addition of four CN groups to (TPP)FeCl. [(CN)$_4$TPP]FeCl has four groups, and $E_{1/2}$ of the first reduction shifts by 510 mV, with respect to (TPP)FeCl. In a similar manner, [[(CN)$_4$TPP]Fe]$_2$O has eight CN groups and shows a shift in $E_{1/2}$ of 870 mV. This suggests that the electron-withdrawing effect of the CN groups is delocalized throughout the whole dimeric system of [[(CN)$_4$TPP]Fe]$_2$O.

Electrode Reactions of [(*p*-Et_2N)TPP]FeCl. The electrooxidation–reduction of [(*p*-Et_2N)TPP]FeCl was investigated in four commonly used electrochemical solvents. These were PhCN, CH_2Cl_2, DMF, and Me_2SO. As will be shown in the following sections, both the number of electrons transferred (in oxidation) and the site of electron transfer (in reduction) appears to be solvent directed.

Figure 7 illustrates typical cyclic voltammograms for the oxidation–reduction of [(*p*-Et_2N)TPP]FeCl in CH_2Cl_2 and DMF (0.1 M TBAP). Two reductions (at E_p = −0.42 V and $E_{1/2}$ = −1.13 V) and four oxidations (at $E_{1/2}$ = 0.61, 0.78, 1.16, and 1.31 V) are observed in CH_2Cl_2 containing 0.1 M TBAP. Similar half-wave potentials were also observed in PhCN containing 0.1 M TBAP, and these values are listed in Table III.

In contrast to results in PhCN or CH_2Cl_2, only three well-defined electrode processes are observed in the potential range of DMF or Me_2SO. This is illustrated in Figure 7b for the reactions of [(*p*-Et_2N)TPP]FeCl in DMF (0.1 M TBAP). As seen in this figure, two one-electron reductions (at E_p = −0.34 V and $E_{1/2}$ = −1.11 V) and a single two-electron oxidation (at $E_{1/2}$ = +0.66 V) are observed. In addition, an irreversible oxidation is also present at the positive oxidation limit of the solvent.

In CH_2Cl_2 or PhCN, [(*p*-Et_2N)TPP]FeCl is oxidized via two one-electron-transfer steps to yield [[(*p*-Et_2N)TPP]FeCl]$^+$ and [[(*p*-Et_2N)TPP]FeCl]$^{2+}$. These reactions occur at 0.61 and 0.78 V and are shown by reactions 5 and 6, respectively. These two

$$[(p\text{-}Et_2N)TPP]FeCl \rightleftarrows [[(p\text{-}Et_2N)TPP]FeCl]^+ + e^- \quad (5)$$

$$[[(p\text{-}Et_2N)TPP]FeCl]^+ \rightleftarrows [[(p\text{-}Et_2N)TPP]FeCl]^{2+} + e^- \quad (6)$$

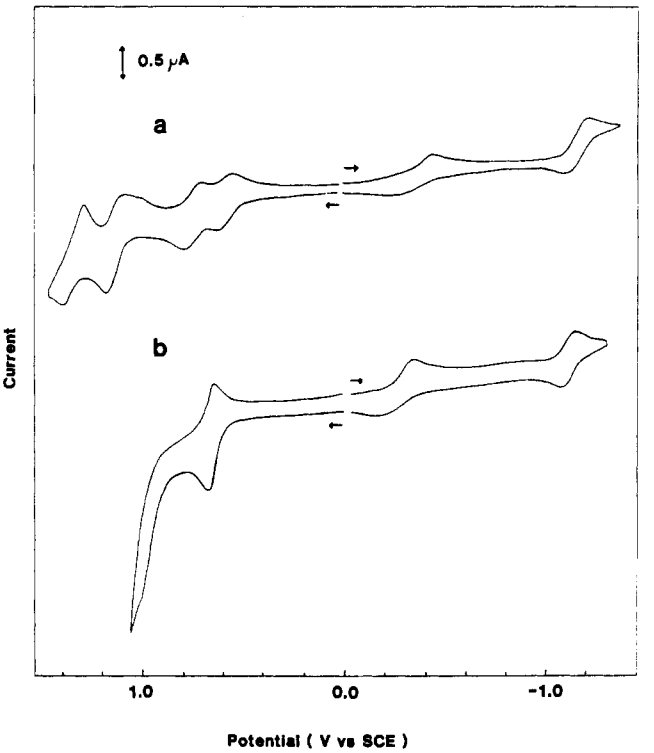

Figure 7. Cyclic voltammograms of [(*p*-Et_2N)TPP]FeCl in (a) CH_2Cl_2 (0.1 M TBAP) and (b) DMF (0.1 M TBAP) [scan rate 100 mV/s].

processes are combined in DMF where the generation of [[(*p*-Et_2N)TPP]FeCl]$^{2+}$ occurs directly via a two-electron oxidation as shown in eq 7.

$$[(p\text{-}Et_2N)TPP]FeCl \rightleftarrows [[(p\text{-}Et_2N)TPP]FeCl]^{2+} + 2e^- \quad (7)$$

The oxidation products of reactions 6 or 7 are identical, and the electrogenerated [[(*p*-Et_2N)TPP]FeCl]$^{2+}$ may be further oxidized to yield [[(*p*-Et_2N)TPP]FeCl]$^{4+}$ and possibly [[(*p*-Et_2N)TPP]FeCl]$^{6+}$. This occurs at 1.16 and 1.31 V in CH_2Cl_2 (see Figure 7a). The oxidation potential limit of DMF is ~1.0 V so that only one irreversible oxidation beyond [[(*p*-Et_2N)-TPP]FeCl]$^{2+}$ is barely seen on the oxidation limit of the solvent (see Figure 7b).

In PhCN or CH_2Cl_2, the first oxidation is spectrally reversible and isosbestic points at 494, 570, and 621 nm are found, indicating the absence of intermediate species. This is shown in Figure 8a, and wavelengths are summarized in Table IV. The large decrease in the Soret band and the appearance of absorption bands in the 700–800 nm region suggest a ring-centered oxidation. This assignment is in accordance with a similar assignment of radical cation formation upon oxidation of (TPP)FeCl.[5] However, the spectrum for [[(*p*-Et_2N)TPP]FeCl]$^+$ in PhCN is quite different from that of [(TPP)FeCl]$^+$ in the same solvent system[30] and more closely resembles that for oxidized [(*p*-Et_2N)TPP]Ni^{II}[31] and

(30) Values of λ ($\epsilon \times 10^{-3}$) in PhCN are as follows for [(TPP)FeCl]$^+$: 407 nm (17.7), 487 (6.6), 539 (5.5).

(31) Chang, D.; Malinski, T.; Ulman, A.; Kadish, K. M. *Inorg. Chem.* **1984**, *23*, 817.

Table IV. Maximum Absorbance Wavelengths (λ_{max}) and Corresponding Molar Absorptivity (ϵ) for Neutral, Oxidized, and Reduced [(*p*-Et_2N)TPP]FeCl Complexes in CH_2Cl_2 (0.5 M TBAP)

species[a]	solvent	λ_{max}, nm ($\epsilon \times 10^{-3}$)				
[(*p*-Et_2N)TPP]FeCl	PhCN	373 (23.8)	453 (51.7)	568 (13.3)	599 (7.9)	747 (3.4)
	CH_2Cl_2	375 (23.5)	453 (51.0)	551 (14.1)	593 sh (6.9)	735 (3.8)
	DMF	377 (22.7)	458 (51.7)	563 (13.1)	595 sh (7.1)	741 (4.1)
$[[(p\text{-}Et_2N)TPP]FeCl]^+$	PhCN	374 (11.5)	471 (25.4)	506 (24.3)	710 (14.3)	773 sh (7.7)
$[[(p\text{-}Et_2N)TPP]FeCl]^{2+}$	PhCN	374 (7.3)	471 (22.2)	561 (21.8)	922 (10.7)[b]	
	DMF[c]	377 (7.3)	470 (22.0)	560 (20.9)	922 (10.5)[b]	
$[[(p\text{-}Et_2N)TPP]FeCl]^{4+}$	PhCN	420 (34.7)	482 (24.9)	659 (7.8)	861 (10.3)	
[(*p*-Et_2N)TPP]Fe]	PhCN	455 (84.5)	546 (6.8)	596 (8.6)	643 sh (6.1)	
	DMF	453 (61.5)	584 (10.0)	627 (10.8)		
$[[(p\text{-}Et_2N)TPP]Fe]^-$	PhCN	379 (16.0)	433 (40.2)	742 sh (2.2)	859 (7.1)	
	DMF	406 sh (31.5)	437 (46.8)	520 (13.3)	621 (7.5)	721 (2.2)

[a] Species indicated assumes loss of anionic ligand during electroreduction. [b] End of the recorded spectrum; the maximum absorbance wavelength in the near-IR region. [c] Species generated from two-electron oxidation of [(*p*-Et_2N)TPP]FeCl.

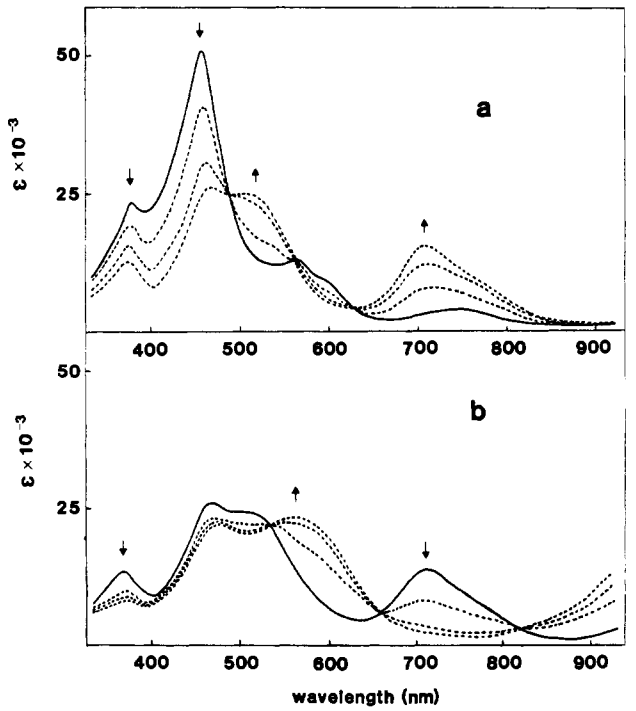

Figure 8. Time-resolved spectra for the stepwise oxidation of [(*p*-Et_2N)TPP]FeCl in PhCN (0.1 M (TBA)PF_6): (a) $[[(p\text{-}Et_2N)TPP]FeCl]^+$ generated at +0.66 V; (b) $[[(p\text{-}Et_2N)TPP]FeCl]^{2+}$ generated at +0.90 V. Initial species are represented by a solid line.

[(*p*-Et_2N)TPP]Ru^{II}(CO)(*t*-Bupy).[32] These latter cation radicals have split Soret bands and large absorbances in the region of 700–900 nm. In addition, a siimilar absorbance peak at 777 nm is observed for $[[[(p\text{-}Et_2N)TPP]Fe]_2O]^+$ in CH_2Cl_2 (0.1 M TBAP) as well as for the $[[(p\text{-}Et_2N)TPP]Cu]^+$ and $[[(p\text{-}Et_2N)TPP]Zn]^+$ radical cations in the same solvent system.[19] Isosbestic points were also observed upon the second one-electron oxidation to yield $[[(p\text{-}Et_2N)TPP]FeCl]^{2+}$. This is shown in Figure 8b. After abstraction of a second electron from [(*p*-Et_2N)TPP]FeCl, the peak at 710 nm disappeared while new absorbances appeared between 820 and 920 nm. This latter wavelength is at the limit of the instrument utilized but suggests a strong absorbance for $[[(p\text{-}Et_2N)TPP]FeCl]^{2+}$ in the IR region. In addition, new broad bands were present between 450 and 600 nm and had spectral maxima at 471 and 561 nm.

The spectrum generated for $[[(p\text{-}Et_2N)TPP]FeCl]^{2+}$ strongly resembles spectra reported for isoporphyrins.[33] However, the stepwise rereduction of $[[(p\text{-}Et_2N)TPP]FeCl]^{2+}$ to [(*p*-Et_2N)TPP]FeCl could be accomplished by the application of a controlled cathodic potential of 0.5 V. Application of these potentials showed first the conversion to $[[(p\text{-}Et_2N)TPP]FeCl]^+$ and then quantitative conversion to the starting species.

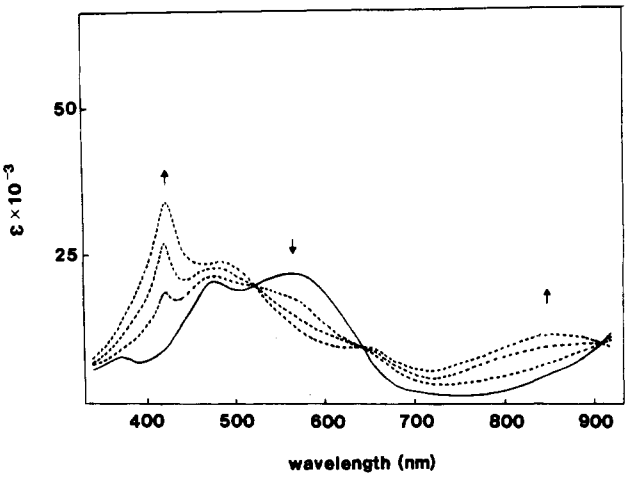

Figure 9. Time-resolved spectra for the two-electron oxidation of $[[(p\text{-}Et_2N)TPP]FeCl]^{2+}$ in PhCN (0.1 M (TBA)PF_6). The initial species is given by a solid line.

Further oxidations of $[[(p\text{-}Et_2N)TPP]FeCl]^{2+}$ in PhCN are proposed to occur at the diethylamino substituents. This postulate is based on the fact that the latter steps involve a two-electron-transfer process that is also observed for all other metalloporphyrin complexes containing the diethylamino substituents. The first of these oxidations occurs at $E_{1/2}$ = 1.14 V and, as seen in Figure 7a, there are coupled peaks that resemble those for an adsorption process. The spectrum of the species generated on this oxidation is shown in Figure 9. Rereduction of the species generated by controlled-potential electrolysis at 1.3 V does not yield $[[(p\text{-}Et_2N)TPP]FeCl]^{2+}$, nor can the initial spectrum of the neutral complex be regenerated. This suggests a coupled chemical reaction of the highly oxidized complex, most likely with the solvent.

Spectral investigations of oxidized [(*p*-Et_2N)TPP]FeCl were also carried out in DMF and Me_2SO. Cyclic voltammetry of [(*p*-Et_2N)TPP]FeCl in DMF gave a diffusion-controlled two-electron-oxidation process as shown in Figure 7b. Values of $(E_{pa} - E_{pc}) = 30 \pm 3$ mV and peak currents for this process were approximately double those for the one-electron reduction of the same compound in PhCN. Similar results were also observed in Me_2SO. The abstraction of 2.0 electrons in DMF or Me_2SO was also verified by controlled-potential coulometry and, in DMF, gave the electronic absorption spectra illustrated in Figure 10. A single isosbestic point was observed at 495 nm, and the electrogenerated species was identical with that observed after the one-electron oxidation of $[[(p\text{-}Et_2N)TPP]FeCl]^+$ in CH_2Cl_2 (see Figure 8 and Table IV). The oxidation in DMF was reversible and the original [(*p*-Et_2N)TPP]FeCl spectrum could be regenerated upon reversing the potential to 0.0 V. No spectral investigations of [(*p*-Et_2N)-

(32) Malinski, T.; Chang, D.; Bottomley, L. A.; Kadish, K. M. *Inorg. Chem.* **1982**, *21*, 4248.
(33) Dolphin, D.; Felton, R. H.; Borg, D. C.; Fajer, J. *J. Am. Chem. Soc.* **1970**, *92*, 743.

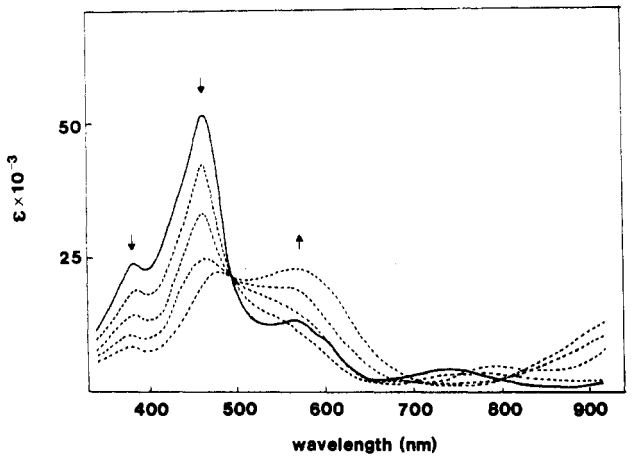

Figure 10. Time-resolved spectra for the overall two-electron oxidation of [(*p*-Et_2N)TPP]FeCl in DMF (0.3 M TBAP) [applied potential +0.90 V]. The initial species is represented by a solid line.

TPP]FeCl were made in Me_2SO because of the compound's very low solubility in this solvent.

The two-electron oxidation of [(*p*-Et_2N)TPP]FeCl in DMF provides the first example where a monomeric iron(III) porphyrin can be reversibly oxidized by two electrons at the same potential. This type of reactivity has been observed for nickel(II) porphyrins,[22] where the orbitals of the π-ring system and the metal system closely overlap[34] as well as for dimeric iron porphyrins where the oxidation occurs at two separate reaction sites.[19] Neither of these cases appears to be operative for [(*p*-Et_2N)TPP]FeCl where dication formation is indicated by the resulting spectra.

Reduction of [(*p*-Et_2N)TPP]FeCl. Potentials for the electrochemical reduction of [(*p*-Et_2N)TPP]FeCl in several solvents are given in Table III and parallel the trend observed for the Fe^{III}/Fe^{II} reaction of (TPP)FeCl.[24,35,36] For both compounds the ease of Fe(III)/Fe(II) reduction follows the order Me_2SO > DMF > CH_2Cl_2 > PhCN. This order relates to an increasing stabilization of Fe(II) by strongly bonding solvents and has been discussed in the literature for the case of (TPP)FeX[24] and (OEP)FeX.[36]

Comparisons between [(*p*-Et_2N)TPP]FeCl and (TPP)FeCl show the expected cathodic shift of $E_{1/2}$ for [(*p*-Et_2N)TPP]FeCl due to the added electron-donating substituents on the complex. This shift ranges from 130 to 160 mV in DMF, PhCN, and CH_2Cl_2, but in Me_2SO, the difference is only 90 mV. It is known that the magnitude of metalloporphyrin substituent effects depends upon the solvent,[37] and this difference is therefore not unexpected.

In all of the studied solvents, the first reduction of [(*p*-Et_2N)TPP]FeCl was irreversible and suggested the electrode reaction shown in eq 8. This reaction involving an EC mechanism

$$[(p\text{-}Et_2N)TPP]FeCl + e^- \rightleftarrows [[(p\text{-}Et_2N)TPP]FeCl]^- \rightleftarrows [(p\text{-}Et_2N)TPP]Fe + Cl^- \quad (8)$$

is typical of numerous iron(III) porphyrins in nonaqueous media[1,2] and gives rise to the type of current–voltage curve shown in Figure 7a for [(*p*-Et_2N)TPP]FeCl in CH_2Cl_2 (0.1 M TBAP).

Spectral studies in different solvents showed a large influence of solvent on the nature of the singly and doubly reduced [(*p*-Et_2N)TPP]FeCl. This is illustrated in Figures 11 and 12 for reduction in PhCN and DMF, respectively. The spectra generated from [(*p*-Et_2N)TPP]FeCl in PhCN (Figure 11) are similar to that of other Fe(II) species in that there is a large increase in the magnitude of the Soret band upon going from Fe(III) to Fe(II). However, in contrast to the reduction of other (TPP)FeX com-

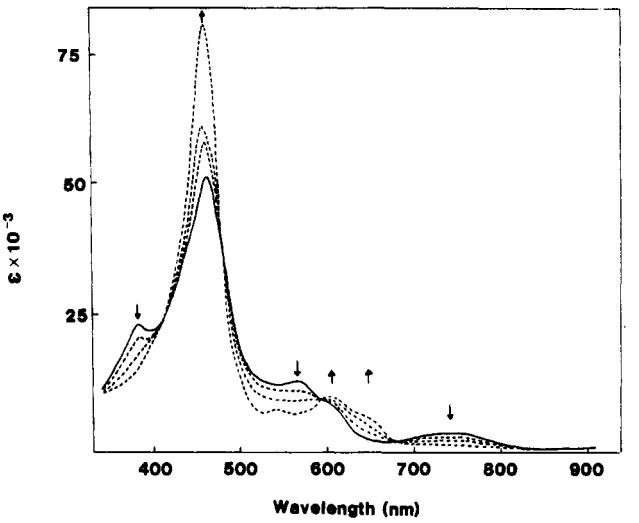

Figure 11. Time-resolved spectra for the first reduction of [(*p*-Et_2N)TPP]FeCl in PhCN (0.1 M $(TBA)PF_6$) [applied potential −0.90 V].

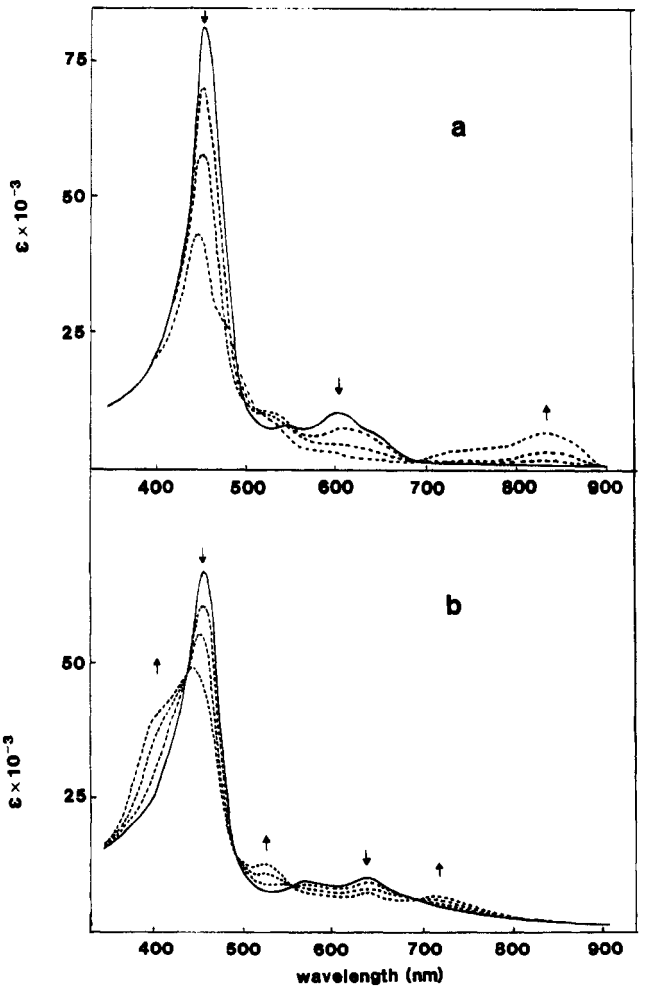

Figure 12. Time-resolved spectra for the second reduction of [(*p*-Et_2N)TPP]FeCl in (a) PhCN (0.1 M $(TBA)PF_6$) and (b) DMF (0.3 M $(TBA)PF_6$) [applied potential −1.40 V]. The initial species is represented by a solid line.

plexes,[38] the Soret band shifts toward the blue upon generation of Fe(II).

The first reduction peak in DMF is also irreversible (Figure 7b) and after controlled-potential electrolysis indicates an Fe(II) species with peaks at 453 (Soret), 584, and 627 nm. This may

(34) Wolberg, A.; Manassen, J. *Inorg. Chem.* **1970**, *9*, 2365.
(35) Kadish, K. M.; Morrison, M. M.; Constant, L. A.; Dickens, L.; Davis, D. G. *J. Am. Chem. Soc.* **1976**, *98*, 8387.
(36) Kadish, K. M.; Bottomley, L. A.; Kelly, S.; Schaeper, D.; Shiue, L. R. *Bioelectrochem. Bioenerg.* **1981**, *8*, 213.
(37) Kadish, K. M.; Morrison, M. M., *Bioelectrochem. Bioenerg.* **1976**, *3*, 480.
(38) Kadish, K. M.; Rhodes, R. K. *Inorg. Chem.* **1983**, *22*, 1090.

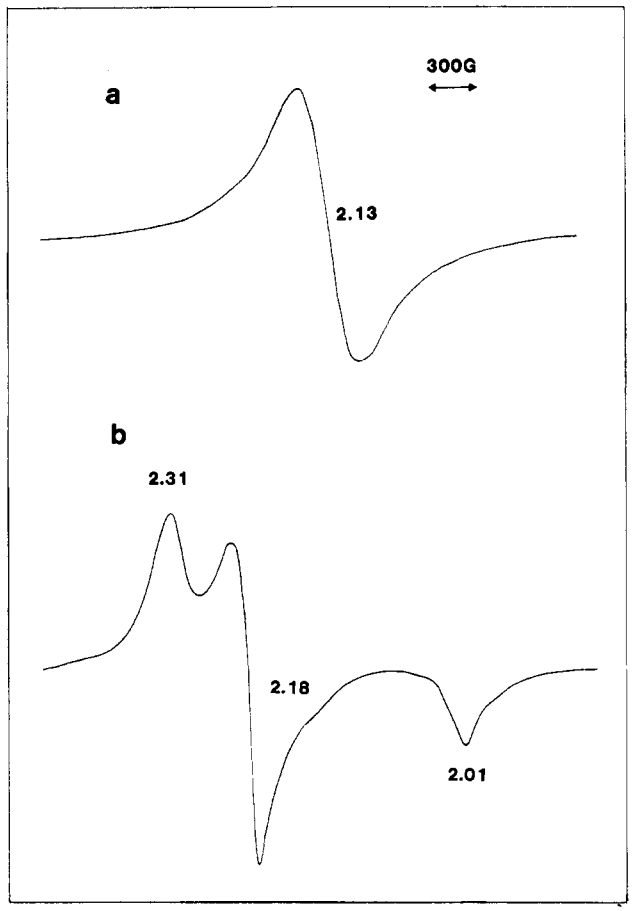

Figure 13. ESR spectra of doubly reduced [(*p*-Et_2N)TPP]FeCl at 110 K in (a) CH_2Cl_2 (0.1 M TBAP) and (b) DMF (0.1 M TBAP) [applied potential −1.50 V].

be contrasted with the spectrum of the singly reduced species in PhCN which has peaks at 455 (Soret), 546, 596, and 643 nm. These differences are not unexpected and may be due to differences in the nature of axial coordination for the Fe(II) species. For the case of (TPP)FeX reduction in CH_2Cl_2, some halide remains coordinated and an equilibrium between five-coordinate $[(TPP)FeX]^-$ and four-coordinate (TPP)Fe is observed.[38] This may not be the case in DMF where predominantly five-coordinate (TPP)Fe(DMF) species are formed.[39,40]

Large solvent effects occur in the spectra of electrogenerated $[[(p\text{-}Et_2N)TPP]Fe]^-$. Reduction in benzonitrile (Figure 12a) leads to a species with a split Soret band at 433 and 474 nm. There is no spectral detail between 550 and 700 nm, but a large absorbance typical of anion radicals occurs at 859 nm. In contrast, the electronic absorption spectra of the doubly reduced species in DMF (Figure 12b) has a split Soret band at 406 and 437 nm, and peaks at 520 and 621 nm are observed in the visible region. The large absorbance at 859 nm in PhCN is not present, and only a small absorbance is noted at 721 nm.

A solvent effect is also observed in the ESR spectra of doubly reduced [(*p*-Et_2N)TPP]FeCl. The ESR spectra were recorded in CH_2Cl_2 and DMF and gave the type of spectra shown in Figure 13. Only one intense and broad signal centered at $g = 2.13$ was observed in CH_2Cl_2. In contrast, the doubly reduced species in DMF exhibits three lines at $g = 2.31$, 2.18, and 2.01. This closely resembles the spectra reported for $[(TPP)Fe]^-$ in DMF[13,14,26] and is in agreement with independent ESR results from another laboratory[41] that clearly identify the species as containing an Fe(I) oxidation state. For comparison purposes, the ESR spectrum of the doubly reduced (TPP)FeCl was also recorded in CH_2Cl_2. The same distortion was observed with *g* values of 2.55, 2.32, and 1.85. One possible explanation for the differences in these ESR spectra could be differences in concentration, or variations in the freezing of the samples. However, in this present case, the experiments with [(*p*-Et_2N)TPP]FeCl were repeated several times, at different concentrations and under different freezing conditions, but always gave the same spectra. Because of this, these differences should not be attributed to a concentration effect nor to the freezing process.

Table V. ESR Values of Doubly Reduced Iron Porphyrins in CH_2Cl_2 at 115 K

complex	$g_\parallel$	$g_\perp$
$[(TPP)Fe]^-$	1.85	2.55, 2.32[a]
$[[(p\text{-}Et_2N)TPP]Fe]^-$		2.13
$[[(CN)_4TPP]Fe]^-$	1.98	2.03, 2.00[a]

[a] Somewhat rhombic.

Effects of the Porphyrin Ring and the Solvent System on the Reduction Site of Fe(II) Complexes. The present study illustrates how electron-donating or electron-withdrawing substituents on a porphyrin ring lead to shifts in potentials for oxidation or reduction of the π-ring system and of the metal center. In addition, the substituents that change the basicity of the conjugated macrocycle may also direct the site of reduction. This is illustrated in Table V where the *g* values of the doubly reduced $[(TPP)Fe]^-$, $[[(p\text{-}Et_2N)TPP]Fe]^-$, and $[[(CN)_4TPP]Fe]^-$ are summarized in CH_2Cl_2. As seen in this table, there is a collapse of both $g_\parallel$ and $g_\perp$ on going from $[(TPP)Fe]^-$ to $[[(p\text{-}Et_2N)TPP]Fe]^-$ to $[[(CN)_4TPP]Fe]^-$. This could be interpreted in terms of differences in energy levels of the e_g orbital of the ring and the d_{z^2}, d_{xz}, and d_{yz} orbitals of the metal. The electron-withdrawing cyano substituents will stabilize the e_g orbitals but would induce an increase of the d_{z^2} energy levels. Hence, the e_g and d_{z^2} would eventually become comparable in energy, and in this case, the distinction between an Fe(I) species and an Fe(II) anion radical would become less clear-cut. This effect would also be observable in the optical spectra of the reduced complexes. For example, the optical spectrum for the monomeric tetracyano complex appears to have characteristics of both a radical and a metal-centered reduction but is more anion radical-like than the spectra of $[(TPP)Fe]^-$ and $[[(p\text{-}Et_2N)TPP]Fe]^-$.

The solvent system may or may not have a marked effect on the reduction site of an iron(II) porphyrin. This seems to depend on the type of porphyrin ring. No effect was noted for $[(TPP)Fe]^-$, and the ESR spectra are identical in DMF and CH_2Cl_2. Both ESR spectra are of a rhombic type, indicative of some distortion. On the other hand, $[[(p\text{-}Et_2N)TPP]Fe]^-$ shows an evolution from a rather rhombic looking spectrum in DMF toward a more axial-like spectrum in CH_2Cl_2. The compound with electron-donating substituents on the porphyrin ring is most likely five-coordinate and probably has the metal out of the porphyrin plane in the noncoordinating solvent. However, in a coordinating solvent like DMF, hexacoordination may occur which would lead to a species having the iron atom more in the porphyrin plane. This could then lead to a distortion of the porphyrin ring.

In conclusion, the present study involves a comparison between monomeric and dimeric iron porphyrin complexes containing either very electron-donating or very electron-withdrawing substituents. It is interesting to note that the most easily reduced monomeric Fe(II) tetracyano complex undergoes a ring-centered reduction and the most easily oxidized Fe(III) complex undergoes a ring-centered oxidation. Thus, in this study, the stabilization of low-valent, or high-valent, iron complexes was not possible by changing the substituents on the porphyrin ring. On the other hand, this study confirms the formulation suggested by Reed,[12] i.e., resonance forms between an iron(I) and an iron(II) radical anion, $[(P)Fe]^-$ and $[(P)Fe^{II}]^{-\cdot}$. It has been suggested[12] that the iron(I) complex is the major contributor to the resonance forms of $[(TPP)Fe]^-$. This is also the case for $[[(p\text{-}Et_2N)TPP]Fe]^-$. In contrast, the iron(II) radical anion seems to be the major contributor to the resonance forms of $[[(CN)_4TPP]Fe]^-$.

(39) Kadish, K. M.; Bottomley, L. A.; Beroiz, D. *Inorg. Chem.* **1978**, *17*, 1124.
(40) Brault, D.; Rougee, M. *Biochemistry* **1974**, *13*, 4591.
(41) Bocian, D. F., private communication.

Acknowledgment. The support of the National Institutes of Health (Grant GM 25172) is gratefully acknowledged. We also acknowledge helpful discussions concerning the ESR spectra with Dr. David Bocian.

Registry No. [[(*p*-Et_2N)TPP]Fe]$_2O$, 89177-90-2; [(*p*-Et_2N)TPP]FeCl, 85529-39-1; [$(CN)_4$TPP]FeCl, 96293-36-6; [[$(CN)_4$TPP]Fe]$_2O$, 69968-24-7; [[$(CN)_4$TPP]Fe]$_2O^-$, 96293-37-7; [[$(CN)_4$TPP]Fe]$_2O^{2-}$, 96293-38-8; [[$(CN)_4$TPP]Fe]$_2O^{3-}$, 96293-39-9; [[$(CN)_4$TPP]Fe]$_2O^{4-}$, 96293-40-2; [(*p*-Et_2N)TPP]FeCl$^+$, 96293-41-3; [(*p*-Et_2N)TPP]FeCl^{2+}, 96293-42-4; [(*p*-Et_2N)TPP]FeCl^{4+}, 96293-43-5; [(*p*-Et_2N)TPP]Fe, 96293-44-6; [(*p*-Et_2N)TPP]Fe$^-$, 96293-45-7; (TPP)Fe$^-$, 54547-68-1; [$(CN)_4$TPP]Fe$^-$, 96293-46-8; [$(CN)_4$TPP]Fe, 96293-47-9; [$(CN)_4$TPP]Fe^{2-}, 96293-48-0; TBAP, 1923-70-2; (TBA)PF_6, 3109-63-5.

Contribution from the Department of Chemistry, Massachusetts Institute of Technology, Cambridge, Massachusetts 02139

Electronic and Vibrational Spectroscopic Analysis of the (μ-Oxo)bis(μ-carboxylato)diiron(III) Core: A Study of $[Fe_2O(O_2CCH_3)_2(TACN)_2]^{2+}$

ALAN SPOOL, IAN D. WILLIAMS, and STEPHEN J. LIPPARD*

Received October 26, 1984

Comparison of the electronic and vibrational spectroscopic properties of the two hemerythrin model compounds $[Fe_2O(O_2CCH_3)_2(TACN)_2]I_2{\cdot}0.5CH_3CN$ (**1**) and $[Fe_2O(O_2CCH_3)_2(HB(pz)_3)_2]$ (**2**) (TACN = 1,4,7-triazacyclononane and $HB(pz)_3^-$ = hydrotris(1-pyrazolyl)borate anion) has enabled identification of features characteristic of the (μ-oxo)bis(μ-carboxylato)diiron(III) core. Raman spectral studies of **1** show ν_s(Fe–O–Fe) to occur at 540 cm^{-1}, shifting to 523 cm^{-1} in [^{18}O]**1**. From difference Fourier transform infrared spectral measurements, the corresponding ν_{as}(Fe–O–Fe) bands were located at 749 cm^{-1} and, for [^{18}O]**1**, 716 cm^{-1}. Electronic spectral transitions between 300 and 500 nm in both **1** and **2** are shown to be diagnostic of the $[Fe_2O(O_2CCH_3)_2]^{2+}$ core. In protic solvents, the optical bands in **1** shift in both frequency and intensity, a result attributed to hydrogen bonding to the oxo bridge. Also reported for **1** are studies of its aqueous solution instability, excitation profiles in the Raman spectrum measured from 454 to 577 nm, and the results of an X-ray crystal structure analysis. The relevance of these studies to the binuclear iron center in hemerythrin is discussed.

Introduction

Recently we prepared and characterized models[1] for the active site of hemerythrin (Hr),[2] the marine invertebrate oxygen transport protein. Our initial objective was to study the (μ-oxo)bis(μ-carboxylato)diiron(III) core, a species identified in the crystal structures of azidomethemerythrin and azidometmyohemerythrin and a likely structure in the bimetallic core of some ribonucleotide reductases (RR).[1,4] An independent report[5] describes the synthesis of a complex containing this same diiron core, but with a capping ligand (1,4,7-triazacyclononane (TACN)) different from the one employed by us, hydrotris(1-pyrazolyl)borate anion ($HB(pz)_3^-$). The resulting cationic complex $[Fe_2O(O_2CCH_3)_2(TACN)_2]^{2+}$ is of similar composition and structure.

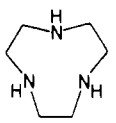

TACN
[9]-ane-N_3

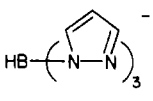

$HB(pz)_3^-$

Among the many physical properties studied for Hr, RR, and related proteins, electronic and vibrational spectra have been most useful in characterizing and identifying the $[Fe_2O(O_2CR)_2]^{2+}$ core. We were therefore interested to learn the degree to which changing the nonbridging ligand from $HB(pz)_3^-$ to TACN would influence these properties in the model compounds. Such a comparison also facilitates assignment of the protein electronic and vibrational spectra. We have therefore undertaken a detailed study of the electronic, resonance Raman and infrared spectra of the (μ-oxo)bis(μ-carboxylato)bis([9]-ane-N_3)diiron(III) cation, the results of which are reported here.

Experimental Section

Materials and Methods. [^{18}O]H_2O (99%) was purchased from Stohler Isotope Chemicals, Waltham, MA. All other reagents, with the exception of the acetonitrile used in the isotope-exchange experiment, were obtained from commerical sources and used without further purification.

Preparation of $[Fe_2O(O_2CCH_3)_2(TACN)_2]I_2{\cdot}0.5CH_3CN$ (1). The complex was prepared as described in the literature,[5] except that in our hands the product of the precipitation with NaI was an orange-brown powder. This material was dissolved in a minimum amount of hot CH_3CN, and the resulting solution was cooled slowly to room temperature. The solution was then allowed to stand at 4 °C for 24 h while brown crystals formed. Since the unit cell and space group of these stable crystals differed from those originally reported,[5] we decided to undertake a complete X-ray structural investigation. The results of this study revealed the presence of acetonitrile in the lattice, which was confirmed by chemical analysis and proton NMR spectroscopy. Anal. Calcd for $Fe_2I_2O_5N_{6.5}C_{17}H_{37.5}$: C, 26.23; H, 4.86; N, 11.69; I, 32.6. Found: C, 25.94; H, 4.95; N, 11.27; I, 34.2. NMR analysis: From the integrated intensity of the proton resonances of a weighed sample of the compound dissolved in CH_3CN-d_3 with $CHCl_3$ as an internal standard, the ratio of acetonitrile molecules to diiron units in compound **1** was measured to be 0.6.

Preparation of [^{18}O][$Fe_2O(O_2CCH_3)_2(TACN)_2$]$I_2$. ^{18}O enrichment of the bridging position in **1** for vibrational spectroscopic studies was accomplished as follows.[1b] Acetonitrile, distilled from calcium hydride under nitrogen, was transferred under nitrogen to a flask containing 50 mg of **1**. After the solid was completely dissolved, 100 μL of [^{18}O]H_2O was syringed into the vessel and the mixture was allowed to stir overnight. The solvent was then removed in vacuo, and the resulting solid was used without further purification. The infrared spectrum of **1** treated in this way with [^{16}O]H_2O was identical with that of the untreated material.

Physical Measurements. ^{1}H NMR spectra were recorded with a Bruker WM 250 spectrometer. Electronic absorption spectra in the range 250–800 nm were recorded with a Cary Model 118C spectropho-

(1) (a) Armstrong, W. H.; Lippard, S. J. *J. Am. Chem. Soc.* **1983**, *105*, 4837–4838. (b) Armstrong, W. H.; Spool, A.; Papaefthymiou, G. C.; Frankel, R. B.; Lippard, S. J. *J. Am. Chem. Soc.* **1984**, *106*, 3653–3667.
(2) (a) Klotz, I. M.; Klippenstein, G. L.; Hendrickson, W. A. *Science (Washington, D.C.)* **1976**, *192*, 335–344. (b) Kurtz, D. M., Jr.; Shriver, D.; Klotz, I. M. *Coord. Chem. Rev.* **1977**, *24*, 145–178. (c) Stenkamp, R. E.; Jensen, L. H. *Adv. Inorg. Biochem.* **1979**, *1*, 219–233. (d) Sanders-Loehr, J.; Loehr, T. M. *Adv. Inorg. Biochem.* **1979**, *1*, 235–252. (e) Wilkins, R. G.; Harrington, P. C. *Adv. Inorg. Biochem.* **1983**, *5*, 51–85. (f) Klotz, I. M.; Kurtz, D. M., Jr. *Acc. Chem. Res.* **1984**, 16–22.
(3) (a) Hendrickson, W. A. In "Invertebrate Oxygen-Binding Proteins: Structure, Active Site, and Function"; Lamy, J., Lamy, J., Eds.; Marcel Dekker: New York, 1981; pp 503–515. (b) Hendrickson, W. A.; Sheriff, S.; Smith, J. L., private communication. (c) Stenkamp, R. E.; Sieker, L. C.; Jensen, L. H.; Sanders-Loehr, J. *Nature (London)* **1981**, *291*, 263–264. (d) Stenkamp, R. E.; Sieker, L. C.; Jensen, L. H. *J. Am. Chem. Soc.* **1984**, *106*, 618–622. (e) Stenkamp, R. E.; Sieker, L. C.; Jensen, L. H. *Acta Crystallogr., Sect. B: Struct. Crystallogr. Cryst. Chem.* **1982**, *B38*, 784–792. (f) Stenkamp, R. E.; Sieker, L. C.; Jensen, L. H. *J. Inorg. Biochem.* **1983**, *19*, 247–253.
(4) (a) Sjöberg, B.-M.; Gräslund, A. *Adv. Inorg. Biochem.* **1983**, *5*, 87–110. (b) Reichard, P.; Ehrenberg, A. *Science (Washington, D.C.)* **1983**, *221*, 514–519. (c) Lammers, M.; Follmann, H. *Struct. Bonding (Berlin)* **1983**, *54*, 27–91.
(5) Wieghardt, K.; Pohl, K.; Gebert, W. *Angew. Chem., Int. Ed. Engl.* **1983**, *22*, 727.

0020-1669/85/1324-2156$01.50/0